Computer Modeling in Engineering & Sciences

Tech Science Press

DOI: 10.32604/cmes.2023.022301

check for updates

ARTICLE

Bifurcation Analysis and Bounded Optical Soliton Solutions of the Biswas-Arshed Model

Fahad Sameer Alshammari[1], Md Fazlul Hoque[2], Harun-Or-Roshid[2] and Muhammad Nadeem[3,*]

[1]Department of Mathematics, College of Science at Alkharj, Prince Sattam bin Abdulaziz University, Alkharj, 11942, Saudi Arabia

[2]Department of Mathematics, Pabna University of Science and Technology, Pabna, 6600, Bangladesh

[3]Faculty of Science, Yibin University, Yibin, 644000, China

*Corresponding Author: Muhammad Nadeem. Email: nadeem@yibinu.edu.cn

Received: 03 March 2022 Accepted: 19 April 2022

ABSTRACT

We investigate the bounded travelling wave solutions of the Biswas-Arshed model (BAM) including the low group velocity dispersion and excluding the self-phase modulation. We integrate the nonlinear structure of the model to obtain bounded optical solitons which pass through the optical fibers in the non-Kerr media. The bifurcation technique of the dynamical system is used to achieve the parameter bifurcation sets and split the parameter space into various areas which correspond to different phase portraits. All bounded optical solitons and bounded periodic wave solutions are identified and derived conforming to each region of these phase portraits. We also apply the extended sinh-Gordon equation expansion and the generalized Kudryashov integral schemes to obtain additional bounded optical soliton solutions of the BAM nonlinearity. We present more bounded optical shock waves, the bright-dark solitary wave, and optical rogue waves for the structure model via these schemes in different aspects.

KEYWORDS

The Biswas-Arshed model; the extended sinh-Gordon equation expansion; the generalized Kudryashov approach; shock wave double solitons; optical singular double solitons; chirp-free bright-dark double solitons

1 Introduction

The study of optical solitons and their applications in the account of optical fiber transmissions is a paramount topic in communication networks. The general concepts of transmission optical solitons in nonlinear optical fiber systems are fundamentally important in controlling optical continuum creation and transferring information over very long distances. The general nonlinear complex models (see [1–7]) are the best examples of the exploration and description of the effect on the picosecond vibration with the group velocity dispersion (GVD) as well as the self-phase modulation (SPM). Such models can be used to explicitly address the electro-magnetic waves with ultrashort pules that can cover the world within a nanosecond. Thus these varieties of waves have been highly studied in the communication technologies, especially, in the optical fibers, data transmissions, telecommunication sectors, transoceanic spaces and so on [6–10]. Recently, Biswas and Arshed introduced a model which is greatly interesting due to the consideration of minor GVD and neglecting the SPM [1]. A number of

works have done on this model to investigate optical solitons by using various approaches such as the trail solution technique [12], modified simple equation technique [13], Kerr and power law nonlinearity [14,15], mapping method [16], the extended trial function method [17], parameter restriction approach [18] and the $tan(\frac{\theta}{2})$ expansion approach [19]. They also pointed out the bright, singular and combo-solitons for the two integration structures of the model. It is fundamentally effective in investigating the dynamical bounded and unbounded solitons in optical fibers and metameterials in case of both low GVD and nonlinearity via new effective approaches. Young dynamical researchers established more new effective schemes to obtain various types of optical solitons like the generalized Kudryashov (GK) approaches [20,21], the Jacobian elliptic function method [22], the extended sinh-Gordon equation expansion method [23], Hirota bilinear scheme [24,25], Darboux transformation method [26], dynamical system approaces [27], solitary waves travel in a porous medium or along an unsmooth boundary [28,29] and so on. Although all those approaches have derived many profound results, some bounded optical wave solutions could still be an unexplored subjects via dynamical scheme with a bifurcation of the BAM.

The purpose of this paper is to show how we can present optical shock wave including both bright and dark, optical soliton solutions, and construct the periodic wave solutions via dynamical system method with bifurcation analysis for the model. We also use the extended sinh-Gordon equation expansion (EShGEE) and the generalized Kudryashov (GK) approaches [20,21] to get a more bounded wave solution. To our knowledge, these types of investigations for the BAM are the first step in the study of the dynamical system, EShGEE and the GK methods.

2 The Biswas-Arshed Model

The Biswas-Arshed model (BAM) [11] is given as the following form:

$$i\Psi_t + a_1\Psi_{xx} + a_2\Psi_{xt} + i(b_1\Psi_{xxx} + b_2\Psi_{xxt}) = i[\varepsilon(|\Psi|^2\Psi)_x + \sigma(|\Psi|^2)_x\Psi + \vartheta|\Psi|^2\Psi_x], \tag{1}$$

where $\Psi(x,t)$ is the wave function of soliton and a_1, a_2, b_1, b_2 are, respectively, the GVD coefficient, the spatio-temporal dispersion, the third-order dispersion coefficient, and the spatio-temporal third-order dispersion coefficient. In the model ε represents self-steepening and σ, ϑ are dispersion effects. Biswas and Arshed first explored this model in the context of higher-order dispersions with minor self-phase modulation. The optical solutions of the model with transmission wave have been retrieved in the point of view of Kerr and non-Kerr law [14]. Recently, the effect of the optical shock wave, optical solitons, rogue waves and their various interactions were investigated in [19]. In this paper, we revisit this model as it has wider applicability, and many other aspects such as bright and dark, optical soliton and the periodic wave solutions of the BAM by the method of a dynamical system with bifurcation analysis, the EShGEE and the GK methods still remain. In the following section, we use the transformation variable to Eq. (1).

2.1 The Structure of BAM

The transformation variable [11]

$$\Psi(x,t) = \Phi(\zeta)e^{i\chi(x,t)}, \tag{2}$$

where $\Phi(\zeta)$ is the amplitude portion with $\zeta = x - \delta t$, the phase component $\chi(x,t) = -kx + wt + \rho$, where the constants δ, ρ, w, k are, respectively, the soliton velocity, the phase constant, the wave number and the frequency of the soliton, convert the nonlinear evaluation Eq. (1) to an ordinary differential

equation. After a long computation and an integration, one can present the differential equation of Eq. (1) [11,14] as follows:

$$(a_1 - a_2\delta + 3b_1k - 2b_2\delta k - b_2w)\Phi'' - (a_1k^2 - a_2wk + b_1k^3 - b_2wk^2 + w)\Phi - k(\varepsilon + \vartheta)\Phi^3 = 0. \quad (3)$$

and the imaginary part:

$$(b_2\delta k^2 - 3b_1k^2 + 2b_2wk - \delta + 2a_2\delta k - 2a_1k + a_2w)\Phi' + (b_1 - b_2\delta)\Phi''' - (2\sigma + \vartheta + 3\varepsilon)\Phi^2\Phi' = 0. \quad (4)$$

One can easily find the following conditions that satisfies the Eq. (4): $\delta = b_1/b_2, b_2\delta k^2 - 3b_1k^2 + 2b_2wk - \delta + 2a_2\delta k - 2a_1k + a_2w = 0$ and $2\sigma + \vartheta + 3\varepsilon = 0$.

Thus, we have to analyze the Eq. (3) only. In the following subsection, we analyze bifurcation to acquire phase portraits to identify the number and types of solutions that exist for the model. Beside this, we apply three different techniques, namely, the dynamical, the EShGEE and the GK approaches to the corresponding model Eq. (3) in order to obtain the corresponding exact optical soliton solutions of Eq. (1).

2.2 Bifurcations Analysis of the BAM

We first consider the bifurcations of phase orbits of ordinary differential equation (ODE) Eq. (3). To proceed of the motive, we need to convert the second order ODE to a dynamical system, which is possible by setting $\Phi' = \Theta$ in the ODE. In this case the ODE in Eq. (3) takes the form of a dynamical system:

$$\Phi' = \Theta,$$

$$\Theta' = \frac{\mathscr{Q}}{\mathscr{P}}\Phi + \frac{\mathscr{R}}{\mathscr{P}}\Phi^3, \quad (5)$$

with the Hamiltonian

$$H(\Phi, \Theta) = \frac{\Theta^2}{2} - \frac{\mathscr{Q}}{2\mathscr{P}}\Phi^2 - \frac{\mathscr{R}}{4\mathscr{P}}\Phi^4, \quad (6)$$

where $\mathscr{P} = a_1 - a_2\delta + 3b_1k - 2b_2\delta k - b_2w$, $\mathscr{Q} = a_1k^2 - a_2wk + b_1k^3 - b_2wk^2 + w$ and $\mathscr{R} = k(\varepsilon + \vartheta)$.

Setting the system of Eq. (5) to zero gives critical points $O(0,0)$, $A(\sqrt{-\frac{\mathscr{Q}}{\mathscr{R}}}, 0)$ and $B(-\sqrt{-\frac{\mathscr{Q}}{\mathscr{R}}}, 0)$. Determinants of Jacobian matrices at the three equilibrium points are: $detJ_O = -\frac{\mathscr{Q}}{\mathscr{P}}$, $detJ_A = \frac{2\mathscr{Q}}{\mathscr{P}}$ and $detJ_B = \frac{2\mathscr{Q}}{\mathscr{P}}$.

If $\frac{\mathscr{Q}}{\mathscr{R}} < 0$, the system has three equilibrium points O, A, B and two cases arise here: (i) $\frac{\mathscr{Q}}{\mathscr{P}} > 0$ implies O-saddle, A, B-centers; there exist two homoclinic orbits Γ^A (right side) and Γ^B (left side) (see the Fig. 1a) that connect at the saddle O. Centers A and B are surrounded by a family of periodic orbits

$$\Gamma^A(h) = \left\{ H(\Phi, \Theta) = h, \qquad h \in \left(\frac{\mathscr{Q}^2}{2\mathscr{R}\mathscr{P}}, 0 \right) \right\}$$

$$\Gamma^B(h) = \left\{ H(\Phi, \Theta) = h, \qquad h \in \left(\frac{\mathscr{Q}^2}{2\mathscr{R}\mathscr{P}}, 0 \right) \right\}. \quad (7)$$

(ii) $\frac{\mathscr{Q}}{\mathscr{P}} < 0$ implies O-center, A, B-saddles. There exist two heteroclinic orbits Γ_u^O (upper) and Γ_L^O (lower) (see the Fig. 1b) that connect at the saddles A, B. Center O is surrounded by a family of periodic orbits.

$$\Gamma^O(h) = \left\{ H(\Phi, \Theta) = h, \qquad h \in \left(0, \frac{\mathscr{Q}^2}{2\mathscr{R}\mathscr{P}}\right) \right\} \tag{8}$$

On the other hand, if $\frac{\mathscr{Q}}{\mathscr{R}} > 0$, the system has only one real equilibrium point at O: (i) for $\frac{\mathscr{Q}}{\mathscr{P}} > 0$ implies O-saddle (see the Fig. 2a), (ii) for $\frac{\mathscr{Q}}{\mathscr{P}} < 0$ implies O-center (see the Fig. 2b).

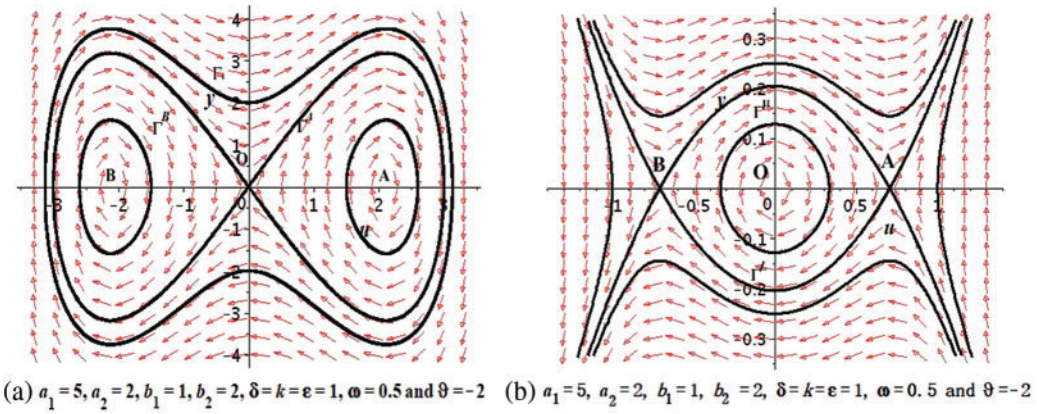

(a) $a_1 = 5, a_2 = 2, b_1 = 1, b_2 = 2, \delta = k = \varepsilon = 1, \varpi = 0.5$ and $\vartheta = -2$ (b) $a_1 = 5,\ a_2 = 2,\ b_1 = 1,\ b_2 = 2,\ \delta = k = \varepsilon = 1,\ \varpi = 0.5$ and $\vartheta = -2$

Figure 1: Bifurcation of system Eq. (5) with $\frac{\mathscr{Q}}{\mathscr{R}} < 0$: (a) for $\frac{\mathscr{Q}}{\mathscr{P}} > 0$ (b) for $\frac{\mathscr{Q}}{\mathscr{P}} < 0$ at $x = t = 1$

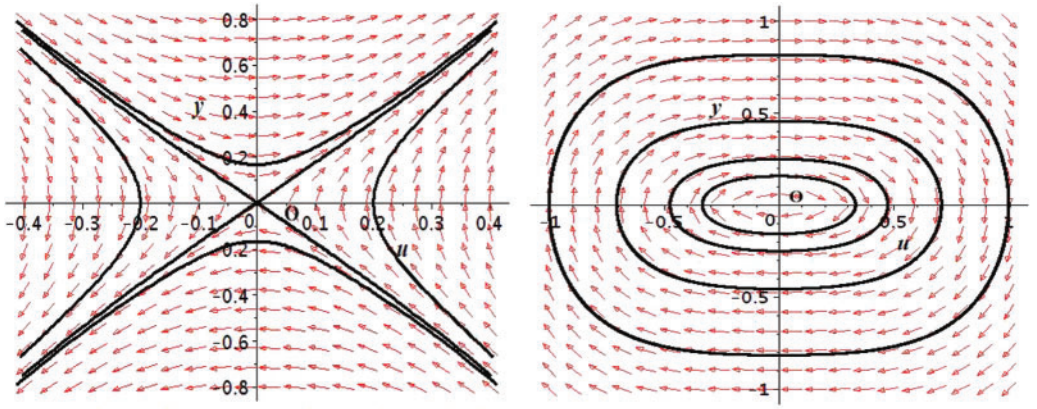

(a) $a_1 = b_1 = a_2 = b_2 = \delta = k = \varepsilon = 1,\ \varpi = 0.5$ and $\vartheta = 2$ (b) $a_1 = b_1 = \delta = k = \varepsilon = 1,\ a_2 = b_2 = \vartheta = 2$ and $\varpi = 0.5$

Figure 2: Bifurcation of system Eq. (5) with $\frac{\mathscr{Q}}{\mathscr{R}} > 0$: (a) for $\frac{\mathscr{Q}}{\mathscr{P}} > 0$ (b) for $\frac{\mathscr{Q}}{\mathscr{P}} < 0$ at $x = t = 1$

Moreover, a different dynamical system can arise for $\mathscr{Q} = 0$, which reads

$$\begin{aligned} \Phi' &= \Theta, \\ \Theta' &= \frac{\mathscr{R}}{\mathscr{P}}\Phi^3, \end{aligned} \tag{9}$$

with the Hamiltonian

$$H(\Phi,\Theta)=\frac{\Theta^2}{2}-\frac{\mathscr{R}}{4\mathscr{P}}\Phi^4. \tag{10}$$

It has a unique critical point $A(0,0)$ of higher order with $det\mathscr{P}=0$. From the theorem-2 of [27], we get $a_{2m+1}=\frac{2\mathscr{R}}{\mathscr{P}}$ and $b_n=0$. It yields that A is a saddle point when $\frac{\mathscr{R}}{\mathscr{P}}>0$ (see the Fig. 3a) and A is a critical point when $\frac{\mathscr{R}}{\mathscr{P}}<0$ (see the Fig. 3b). We observe that all bounded orbits and traveling wave solutions can be simulated on the phase portraits. All bounded orbits and travelling wave solutions can be simulated.

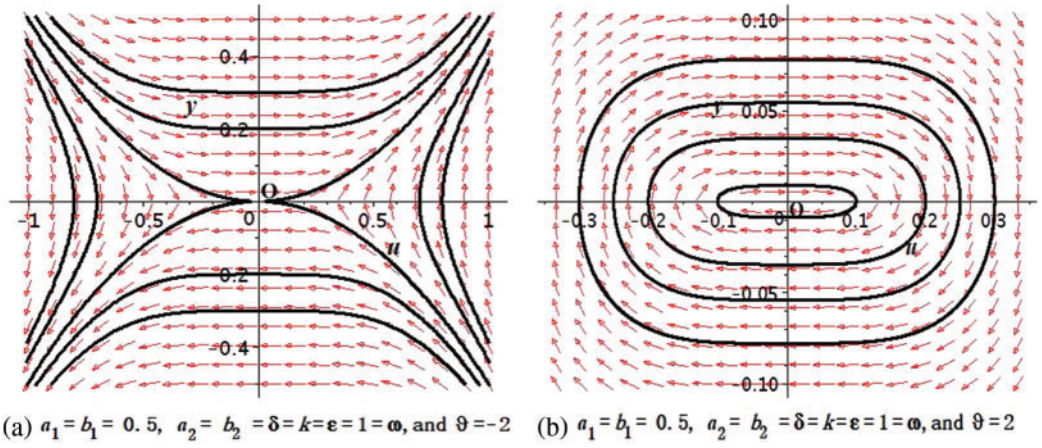

(a) $a_1=b_1=0.5$, $a_2=b_2=\delta=k=\varepsilon=1=\omega$, and $\vartheta=-2$ (b) $a_1=b_1=0.5$, $a_2=b_2=\delta=k=\varepsilon=1=\omega$, and $\vartheta=2$

Figure 3: Bifurcation of system Eq. (5) with $\mathscr{Q}=0$: (a) for $\frac{\mathscr{Q}}{\mathscr{P}}>0$ (b) for $\frac{\mathscr{Q}}{\mathscr{P}}<0$ at $x=t=1$

2.3 Bounded Travelling Wave Solutions of BAM

This section will provide the explicit expressions of all bounded travelling wave solution of the system Eq. (5).

2.3.1 The Periodic Wave Solution

Recall the cases $\frac{\mathscr{Q}}{\mathscr{R}}<0$ and $\frac{\mathscr{Q}}{\mathscr{P}}>0$, there are two classes of periodic orbits Γ^A and Γ^B enclosing A and B, respectively. The corresponding wave solutions via Eq. (6) closed orbit Γ^A are as follows:

$$\Theta=\pm\sqrt{\frac{-\mathscr{R}}{2\mathscr{P}}}\sqrt{(\Phi-l)(\Phi-m)(\Phi-n)(r-\Phi)}, \tag{11}$$

where $l<m<n<\Phi<r$. Let us consider the periodicity of the orbit is $2T_1$ and initial value $\Phi(0)=n$, we have

$$\int_n^{\Phi}\sqrt{-\frac{2\mathscr{P}}{\mathscr{R}}}\frac{d\Phi}{\sqrt{(\Phi-l)(\Phi-m)(\Phi-n)(r-\Phi)}}=\int_0^{\zeta}d\zeta;\qquad 0<\zeta<T_1. \tag{12}$$

$$-\int_{\Phi}^{n}\sqrt{-\frac{2\mathscr{P}}{\mathscr{R}}}\frac{d\Phi}{\sqrt{(\Phi-l)(\Phi-m)(\Phi-n)(r-\Phi)}}=\int_{\zeta}^{0}d\zeta;\qquad -T_1<\zeta<0. \tag{13}$$

Combining Eqs. (12) and (13), it leads to

$$\int_n^{\Phi} \sqrt{-\frac{2\mathscr{P}}{\mathscr{R}}} \frac{d\Phi}{\sqrt{(\Phi-l)(\Phi-m)(\Phi-n)(r-\Phi)}} = |\zeta|. \tag{14}$$

By the direct elliptic integral and calculation, we arrive at the solution

$$\Phi_1(\zeta) = m + (n-m)(r-m)\{(r-m) - (r-n)sn^2(\sqrt{\frac{-\mathscr{R}}{2\mathscr{P}}} \frac{\sqrt{(r-m)(n-l)}}{2}|\zeta|)\}^{-1}, \tag{15}$$

where $T_1 = \dfrac{2b_2\pi}{b_1\sqrt{((r-m)(n-l))}}\sqrt{-\dfrac{2\mathscr{P}}{\mathscr{R}}}$. Noting that

$$\int_n^{\Phi} \frac{d\Phi}{\sqrt{(\Phi-l)(\Phi-m)(\Phi-n)(r-\Phi)}} = \kappa sn^{-1}(\sqrt{\frac{(r-m)(\Phi-n)}{(r-n)(\Phi-m)}}, \beta), \tag{16}$$

where $\kappa = 2/\sqrt{(r-m)(n-l)}$ and $\beta^2 = (r-n)(m-l)/((r-m)(n-l))$. Now, the corresponding bounded periodic optical wave solution is coming from the relation Eq. (2) with modulus $|\Psi_1(x,t)|$.

Similarly, the periodic solution corresponding to Γ^B can be expressed as

$$\Theta = \pm\sqrt{\frac{-\mathscr{R}}{2\mathscr{P}}}\sqrt{(\Phi-l)(m-\Phi)(n-\Phi)(r-\Phi)}, \tag{17}$$

where $l < \Phi < m < n < r$. Taking period is $2T_2$ and initial condition $\Phi(0) = l$, we arrive at the solution

$$\Phi_2(\zeta) = r - (r-m)(r-l)\{(r-m) + (m-l)sn^2(\sqrt{\frac{-\mathscr{R}}{2\mathscr{P}}} \frac{\sqrt{(r-m)(r-l)}}{2}|\zeta|)\}^{-1}, \tag{18}$$

where $\kappa = 2/\sqrt{(r-m)(n-l)}$ and $\beta^2 = (r-n)(m-l)/((r-m)(n-l))$, and $T_2 = \dfrac{2b_2\pi}{b_1\sqrt{((r-m)(r-l))}}\sqrt{-\dfrac{2\mathscr{P}}{\mathscr{R}}}$. Now, the corresponding bounded periodic wave are coming from the relation Eq. (2) with modulus $|\Psi_2(x,t)|$.

Again, recall the cases $dfrac\mathscr{Q}\mathscr{R} < 0$ and $\dfrac{\mathscr{Q}}{\mathscr{P}} < 0$, there is class of periodic orbits Γ^O enclosing O. The corresponding wave solutions via Eq. (6) closed orbit Γ^O are as follows:

$$\Theta = \pm\sqrt{\frac{\mathscr{R}}{2\mathscr{P}}}\sqrt{(\Phi-l)(\Phi-m)(n-\Phi)(r-\Phi)}, \tag{19}$$

where $l < m < \Phi < n < r$ which are real valued constants. Let us consider the periodicity of the orbit is $2T_3$ and initial value $\Phi(0) = m$, we obtain

$$\int_m^{\Phi} \sqrt{\frac{2\mathscr{P}}{\mathscr{R}}} \frac{d\Phi}{\sqrt{(\Phi-l)(\Phi-m)(n-\Phi)(r-\Phi)}} = \int_0^{\zeta} d\zeta; \qquad 0 < \zeta < T_3. \tag{20}$$

$$-\int_{\Phi}^{m} \sqrt{\frac{2\mathscr{P}}{\mathscr{R}}} \frac{d\Phi}{\sqrt{(\Phi-l)(\Phi-m)(n-\Phi)(r-\Phi)}} = \int_{\zeta}^{0} d\zeta; \qquad -T_3 < \zeta < 0. \tag{21}$$

Combining Eqs. (20) and (21), it leads to

$$\int_m^{\Phi} \sqrt{\frac{2\mathscr{P}}{\mathscr{R}}} \frac{d\Phi}{\sqrt{(\Phi-l)(\Phi-m)(n-\Phi)(r-\Phi)}} = |\zeta|. \tag{22}$$

Again by the elliptic integral and after some calculation, we arrive at the solution

$$\Phi_3(\zeta) = l + (n-l)(m-l)\{(n-l) - (n-m)sn^2(\sqrt{\frac{\mathscr{R}}{2\mathscr{P}}} \frac{\sqrt{(r-m)(n-l)}}{2}|\zeta|)\}^{-1}, \tag{23}$$

where $T_3 = \dfrac{2b_2\pi}{b_1\sqrt{((r-m)(n-l))}}\sqrt{\dfrac{2\mathscr{P}}{\mathscr{R}}}$. Noting that

$$\int_m^{\Phi} \frac{d\Phi}{\sqrt{(\Phi-l)(\Phi-m)(n-\Phi)(r-\Phi)}} = \kappa sn^{-1}(\sqrt{\frac{(n-l)(\Phi-m)}{(n-m)(\Phi-l)}}, \beta), \tag{24}$$

where $\kappa = 2/\sqrt{(r-m)(n-l)}$ and $\beta^2 = (n-m)(r-l)/((r-m)(n-l))$. Now, corresponding bounded periodic wave are coming from the relation Eq. (2) with modulus $|\Psi_3(x,t)|$. It is noted that three classes of periodic wave solutions of the Eq. (5) specified by $\Phi_i(x,t); i = 1,2,3$ are achieved for different regions and the corresponding optical waves, which are specified by $|\Psi_i(x,t)|, i = 1,2,3$. Since the nature of the waves are similar but in different boundary area with different initial conditions, we depicted only the $\Phi_1(x,t)$ and $\Psi_1(x,t)$ graphically in the Fig. 4. To investigate all the propagation properties of the wave, we illustrate here the 3D plots of $\Phi_1(x,t)$, real part, imaginary part and square of modulus of $|\Psi_1(x,t)|$ in Figs. 4a–4d, respectively.

2.3.2 The Solitary Wave Solutions

Using the cases $\dfrac{\mathscr{Q}}{\mathscr{R}} < 0$ and $\dfrac{\mathscr{Q}}{\mathscr{P}} > 0$, the homoclinic orbits Γ^A and Γ^B can be represented as

$$\Theta = \pm\sqrt{\frac{-\mathscr{R}}{2\mathscr{P}}}\sqrt{(\Phi+l)\Phi^2(l-\Phi)}, \tag{25}$$

where $-l < \Phi < l$. Setting the homoclinic orbit and initial value $\Phi(0) = m$, we obtain

$$\int_{\Phi}^{l} \sqrt{-\frac{2\mathscr{P}}{\mathscr{R}}} \frac{d\Phi}{\Phi\sqrt{(\Phi+l)(l-\Phi)}} = -|\zeta|. \tag{26}$$

Applying the elliptic integral and some calculation, we arrive at the solution

$$\Phi_4(\zeta) = \frac{2lexp(\sqrt{\dfrac{-\mathscr{R}}{2\mathscr{P}}}m|\zeta|)}{1+exp(2\sqrt{\dfrac{-\mathscr{R}}{2\mathscr{P}}}m|\zeta|)}, l > 0. \tag{27}$$

The resulting solution Φ_4 comes due to the homoclinic orbit Γ^A for the system Eq. (5) by (6) and it expresses the bright peaked soliton, i.e., bright peakon. Now, the corresponding bounded optical soliton solution will come through the relation Eq. (2) with modulus as $|\Psi_4(x,t)|$, which is also a bright optical peakon soliton.

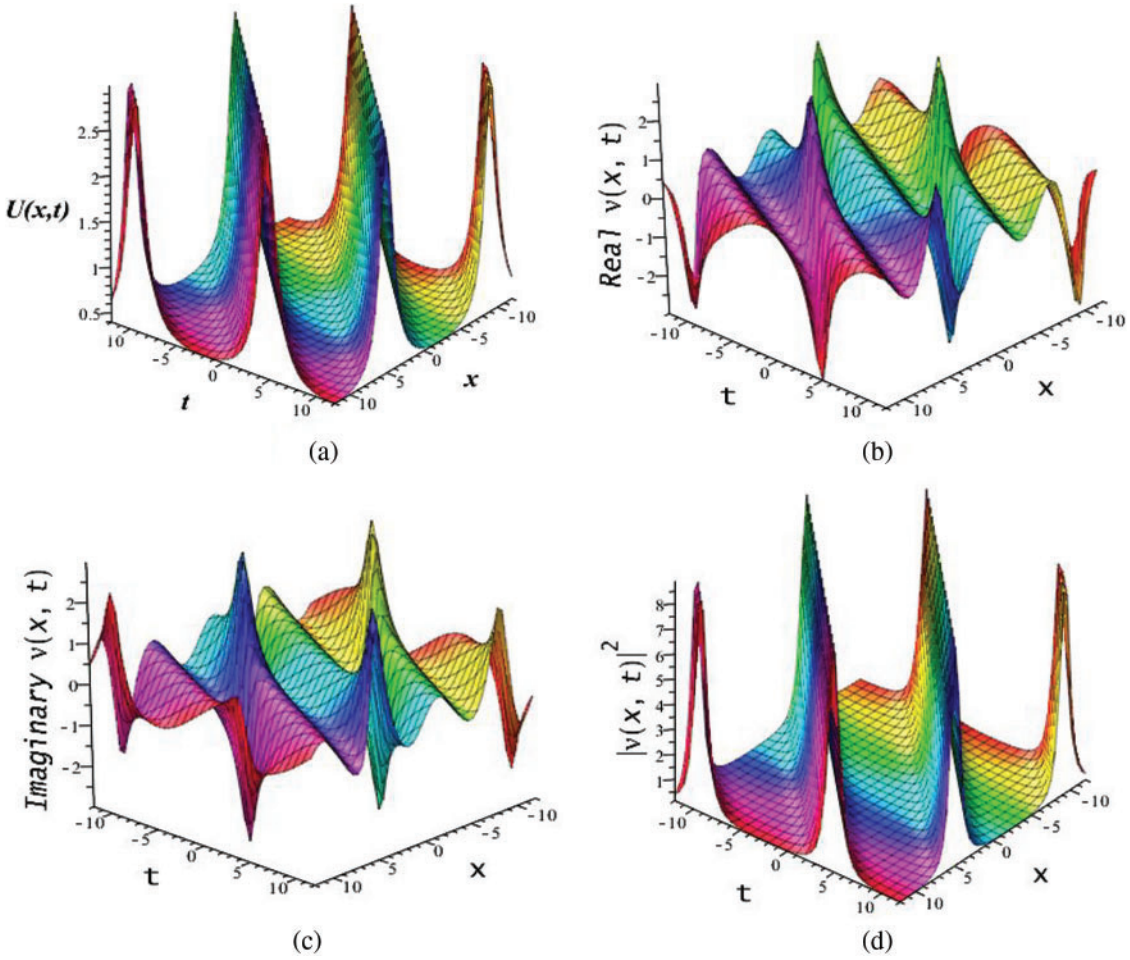

Figure 4: (a) Periodic wave for + via Eq. (15), (b) real part of $\Psi_1(x,t)$ for Eq. (15), (c) imaginary part of $\Psi_1(x,t)$ for Eq. (15) and (d) optical bright waves $|\Psi_1(x,t)|^2$ for the parametric values $a_1 = 5, a_2 = b_2 = 2, b_1 = \delta = k = \varepsilon = 1, w = 0.5, \vartheta = -2, l = 0.2, m = 0.3, n = 0.4, r = 3$

Similarly, let the homoclinic orbit and initial value $\Phi(0) = -m$, we obtain

$$\int_{-l}^{\Phi} \sqrt{-\frac{2\mathscr{P}}{\mathscr{R}}} \frac{d\Phi}{\Phi\sqrt{(\Phi+l)(l-\Phi)}} = |\zeta|. \tag{28}$$

Through the elliptic integral and after some calculation, we arrive at the solution

$$\Phi_5(\zeta) = \frac{-2le^{\sqrt{\frac{-\mathscr{R}}{2\mathscr{P}}}^{m|\zeta|}}}{1+e^{2\sqrt{\frac{-\mathscr{R}}{2\mathscr{P}}}^{m|\zeta|}}}, \qquad l > 0. \tag{29}$$

The obtained solution Φ_5 comes due to the homoclinic orbit Γ^B for the system Eq. (5) by Eq. (6) and it expresses the dark peaked soliton, i.e., anti-peakon. Now, the corresponding bounded optical soliton solution will arise through the relation Eq. (2) with modulus as $|\Psi_5(x,t)|$, which is also a

bright optical peakon soliton. The nature of the peaked solitons and its optical peaked solitons are demonstrated via the Figs. 5 and 6 for $\Phi_4(x,t)$, $\Psi_4(x,t)$ and $\Phi_4(x,t)$, $\Psi_4(x,t)$ respectively. To investigate the all propagation properties of the wave, we illustrate here the 3D plots of $\Phi_4(x,t)$, $\Phi_5(x,t)$, real part, imaginary part and square of modulus of $|\Psi_4(x,t)|$, $|\Psi_5(x,t)|$ in Figs. 5 and 6a–6d, respectively.

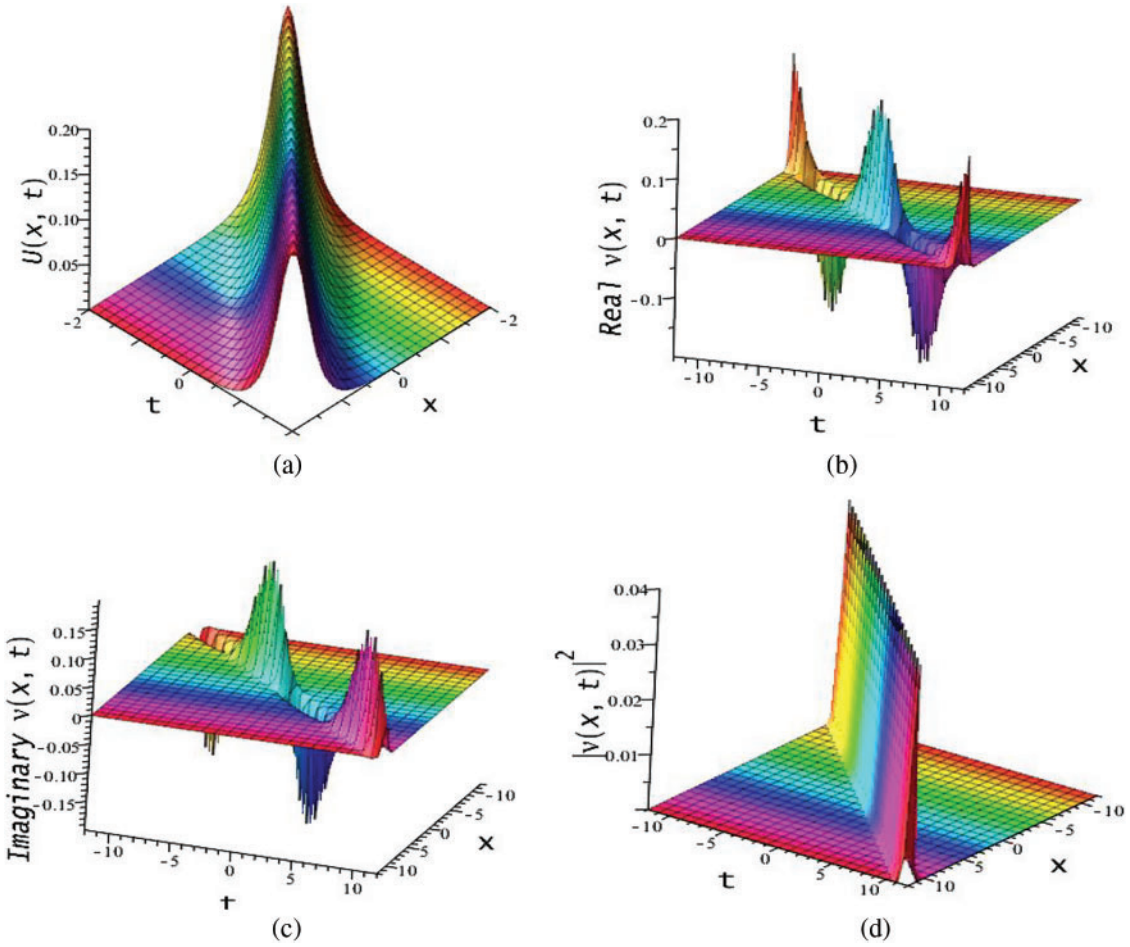

Figure 5: (a) Bright peaked soliton via Eq. (27), (b) Real part of $\Psi_4(x,t)$ for Eq. (27), (c) Imaginary part of $\Psi_4(x,t)$ for Eq. (27) and (d) Optical bright peaked soliton $|\Psi_4(x,t)|^2$ for the parametric values $a_1 = 5, a_2 = b_2 = 2, b_1 = \delta = k = \varepsilon = 1, w = 0.5, \vartheta = -2, l = 0.2, m = 5$

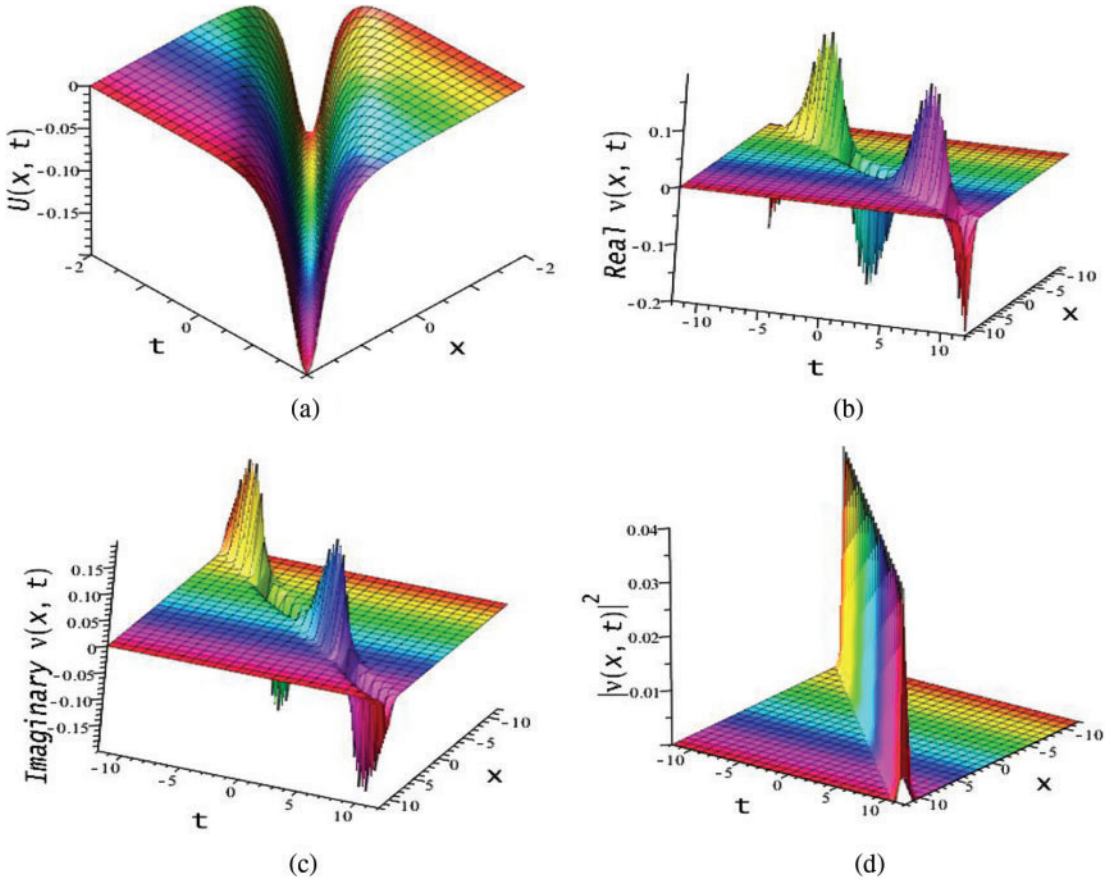

Figure 6: (a) Dark peaked soliton via Eq. (29), (b) Real part of $\Psi_4(x,t)$ for Eq. (29), (c) Imaginary part of $\Psi_4(x,t)$ for Eq. (29) and (d) Optical bright peaked soliton $|\Psi_4(x,t)|^2$ for the parametric values $a_1 = 5, a_2 = b_2 = 2, b_1 = \delta = k = \varepsilon = 1, w = 0.5, \vartheta = -2, l = 0.2, m = 5$

2.3.3 The Shock Wave Solutions

For the cases $\frac{\mathscr{Q}}{\mathscr{R}} < 0$ and $\frac{\mathscr{Q}}{\mathscr{P}} < 0$, the heteroclinic orbits Γ^{μ} and Γ^{L} can be represented as

$$\Theta = \pm\sqrt{\frac{\mathscr{R}}{2\mathscr{P}}}\sqrt{(\Phi - l)^2(r - \Phi)^2}, \tag{30}$$

where $-\sqrt{\frac{-\mathscr{Q}}{\mathscr{R}}} = l < \Phi < r = \sqrt{\frac{-\mathscr{Q}}{\mathscr{R}}}$. For the heteroclinic orbit and initial value $\Phi(0) = \frac{l+r}{2} = 0$, we obtain

$$\int_0^{\Phi} \sqrt{\frac{2\mathscr{P}}{\mathscr{R}}} \frac{d\Phi}{(\Phi - l)(r - \Phi)} = \int_0^{\zeta} d\zeta; \qquad -\infty < \zeta < +\infty. \tag{31}$$

$$-\int_0^{\Phi} \sqrt{\frac{2\mathscr{P}}{\mathscr{R}}} \frac{d\Phi}{(\Phi - l)(r - \Phi)} = \int_0^{\zeta} d\zeta; \qquad -\infty < \zeta < +\infty, \tag{32}$$

and applying the elliptic integral and after some calculation, we arrive at the solution

$$\Phi_6(\zeta) = \frac{r-l}{2} tanh(\frac{r-l}{2}\sqrt{\frac{\mathscr{R}}{2\mathscr{P}}}\zeta), \Phi_7(\zeta) = \frac{r-l}{2} tanh(\frac{l-r}{2}\sqrt{\frac{\mathscr{R}}{2\mathscr{P}}}\zeta) \tag{33}$$

Noting that

$$\int_0^{\Phi} \frac{d\Phi}{(\Phi-l)(\Phi-r)} = \frac{2}{r-l} tanh^{-1}(\frac{2\Phi-(l+r)}{r-l}). \tag{34}$$

The resulting solution $\Phi_6(x,t)$ comes in-terms of *tanh*-function due to the heteroclinic orbit Γ^{μ} for the system Eq. (5) by Eq. (6) and it expresses the kink type shock wave, and its corresponding bounded optical soliton solution will arise through the relation Eq. (2) with modulus as $|\Psi_6(x,t)|$, which is a bounded optical dark peaked soliton, i.e., anti-peakon. The nature of this soliton is specified in Figs. 7a and 7b for $\Phi_6(x,t)$ and $|\Psi_6(x,t)|^2$, respectively. Moreover, the resulting solution $\Phi_7(x,t)$ (depicted in 7c) comes in-terms of *tanh*-function due to the heteroclinic orbit Γ^{L} for the system Eq. (5) by Eq. (6), and it expresses the anti-kink type shock wave and its corresponding bounded optical soliton solution comes through the relation Eq. (2) with modulus as $|\Psi_7(x,t)|^2$ (depicted in Fig. 7d), which is also a bounded optical dark peaked soliton, i.e., anti-peakon.

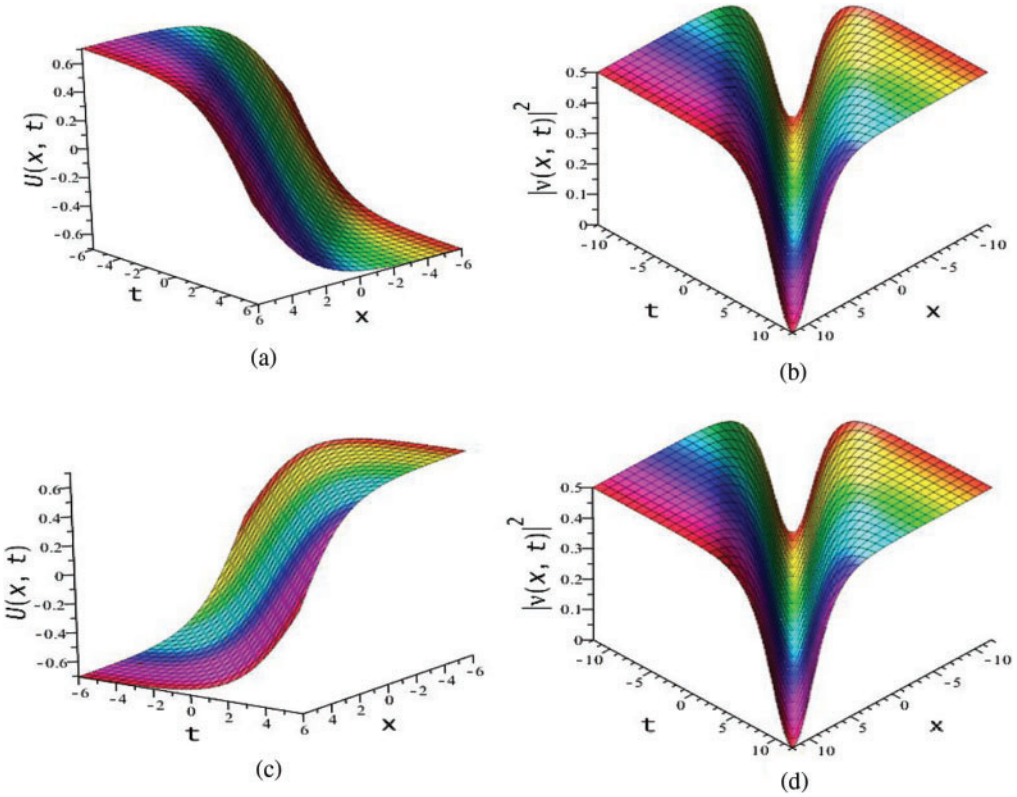

Figure 7: (a) Shock wave (kink) via $\Phi(x,t)$ for Eq. (33), (b) Optical anti-peakon $|\Psi_6(x,t)|^2$ for Eq. (29), (c) Shock wave (anti-kink) via $\Phi(x,t)$ for Eq. (29) and (d) Optical anti-peakon $|\Psi_7(x,t)|^2$ for the parametric values $a_1 = b_1 = \delta = k = \varepsilon = 1, a_2 = b_2 = 2, w = 0.5, \vartheta = -2$

2.4 Optical Soliton Solutions to BAM via the EShGEE

One considers the general form of the trail solution in the extended sinh-Gordon equation expansion approach (EShGEE) [23],

$$\Psi(\ominus) = \sum_{r=1}^{n} \cosh^{r-1}(\ominus)[L_r \sinh(\ominus) + M_r \cosh(\ominus)] + M_0, \tag{35}$$

where M_0, M_r, L_r, $r = 1, 2, \ldots, n$ are free constants to be later calculated, and the $\ominus$ is a function of ζ, which satisfies the condition,

$$\frac{d\ominus}{d\zeta} = \sinh(\ominus). \tag{36}$$

Due to balance principal, the value n of Eq. (35) can be obtained. The Eq. (36) has been obtained from the sinh-Gordon equation [23],

$$u_{xt} = \lambda \sinh(u), \tag{37}$$

and they [23] obtained the solutions,

$$\sinh(\ominus) = \pm csch(\zeta), \quad \text{or} \quad \sinh(\ominus) = \pm isech(\zeta), \tag{38}$$

and

$$\cosh(\ominus) = \pm coth(\zeta), \quad \text{or} \quad \cosh(\ominus) = \pm tanh(\zeta), \tag{39}$$

where $i = \sqrt{-1}$.

We now compute the balance number of Eq. (3), which leads to $n = 1$. Then the trail solution Eq. (35) in the EShGEEM takes the form,

$$\Phi(\ominus) = L_1 \sinh(\ominus) + M_1 \cosh(\ominus) + M_0. \tag{40}$$

Putting Eq. (40) into Eq. (3) along with Eq. (36), we obtain a polynomial of $\sinh(\zeta)$ and $\cosh(\zeta)$ functions, whose equating coefficients lead to a system of equations, and the solutions of the system of equations yield the following constraints:

$$\text{Set 1:} \quad \begin{aligned} \delta &= \frac{-\Gamma_1}{2(k^2 b_2 + k a_2 - 1)(2k b_2 + a_2)}, \\ w &= \frac{k(\varepsilon M_1^2 + k^2 b_1 + \vartheta M_1^2 + k a_1)}{(k^2 b_2 + k a_2 - 1)}, \\ M_0 &= 0, \quad L_1 = 0, \quad M_1 \quad \text{const.}, \end{aligned} \tag{41}$$

$$\text{Set 2:} \quad \begin{aligned} \delta &= \frac{-\Gamma_2}{(k^2 b_2 + k a_2 - 1)(2k b_2 + a_2)}, \\ w &= \frac{k(\varepsilon M_1^2 + k^2 b_1 + \vartheta M_1^2 + k a_1)}{k^2 b_2 + k a_2 - 1}, \\ M_0 &= 0, \quad L_1 = M_1, M_1 \quad \text{const.}, \end{aligned} \tag{42}$$

$$\text{Set 3:} \quad \delta = \frac{-\Gamma_2}{(k^2b_2 + ka_2 - 1)(2kb_2 + a_2)},$$
$$w = \frac{k(\varepsilon M_1^2 + k^2b_1 + \vartheta M_1^2 + ka_1)}{k^2b_2 + ka_2 - 1},$$
$$M_0 = 0, \quad L_1 = -M_1, \tag{43}$$

where M_1 presents arbitrary constant and $\Gamma_1 = (\varepsilon k^3 M_1^2 b_2 + k^3\vartheta M_1^2 b_2 + \varepsilon k^2 M_1^2 a_2 + k^2\vartheta M_1^2 a_2 + 2\varepsilon k M_1^2 b_2 - 4k^3 b_1 b_2 + 2k\vartheta M_1^2 b_2 - \varepsilon k M_1^2 - 6k^2 a_2 b_1 - k\vartheta M_1^2 - 2ka_1 a_2 + 6b_1 k + 2a_1)$, and $\Gamma_2 = 2\varepsilon k^3 M_1^2 b_2 + 2k^3\vartheta M_1^2 b_2 + 2\varepsilon k^2 M_1^2 a_2 + 2k^2\vartheta M_1^2 a_2 + \varepsilon k M_1^2 b_2 - 2k^3 b_1 b_2 + k\vartheta M_1^2 b_2 - 2\varepsilon k M_1^2 - 3k^2 a_2 b_1 - 2k\vartheta M_1^2 - ka_1 a_2 + 3kb_1 + a_1$.

Now for the Set 1, if we combine Eq. (41) with Eqs. (38)–(40), and substituting into Eq. (2), we obtain the exact soliton solutions of Eq. (1). These solutions of the model give us the optical shock wave and optical singular shock solitons,

$$\Psi_{8,9}(x,t) = \pm M_1 \tanh(x - \delta t) e^{i(-kx+wt+\rho)}, \tag{44}$$

$$\Psi_{10,11}(x,t) = \pm M_1 \coth(x - \delta t) e^{i(-kx+wt+\rho)}, \tag{45}$$

where δ and w come from Eq. (41). In the Eq. (44), $\Phi(x,t)$ comes in terms of *tanh*-function which presents kink shock waves. This solution presents a kink shock wave for the positive taking sign in the results (see Fig. 8a) but taking negative sign it presents an anti-kink shock wave (see Fig. 8b). The corresponding optical solitons represent dark-bell type peaked soliton (see Fig. 8c). On the other hand, in the Eq. (45), $\Phi(x,t)$ comes in terms of *coth*-function which presents kink shock waves with singularities i.e., singular kink type shock wave, for the positive sign it expresses singular kink but for the negative sign, it presents singular anti-kink type shock wave. The corresponding optical solitons represent bright peaked solitons with singularities (see Fig. 8d).

Similarly, for the Set 2, if we combine Eq. (42) with Eqs. (38)–(40), and substituting into Eq. (2), we obtain the exact soliton solutions of Eq. (1). These solutions give us the combination of chirp-free bright and optical shock wave double solitons, and the combination of optical singular double solitons,

$$\Psi_{12,13}(x,t) = M_1[\pm isech(x - \delta t) \pm \tanh(x - \delta t)] e^{i(-kx+wt+\rho)}, \tag{46}$$

$$\Psi_{14,15}(x,t) = M_1[\pm csch(x - \delta t) \pm \coth(x - \delta t)] e^{i(-kx+wt+\rho)}, \tag{47}$$

where δ and w come from Eq. (42). And for the Set 3, if we combine Eq. (43) with Eqs. (38)–(40), and substituting into Eq. (2), we obtain the exact soliton solutions of Eq. (1). These solutions are able to give the combination of chirp-free bright and optical shock wave double solitons, and the combination of optical singular double solitons,

$$\Psi_{16,17}(x,t) = M_1[\mp isech(x - \delta t) \pm \tanh(x - \delta t)] e^{i(-kx+wt+\rho)}, \tag{48}$$

$$\Psi_{18,19}(x,t) = M_1[\mp csch(x - \delta t) \pm \coth(x - \delta t)] e^{i(-kx+wt+\rho)}, \tag{49}$$

where δ and w come from Eq. (43). The nature of solutions $\Psi_{12,13}(x,t)$ and $\Psi_{16,17}(x,t)$ are similar as they comes from produce periodic exponential function with linear combinations of *sech*-function (give bell solitonic nature) and *tanh*-function (give kink shock solitonic nature). Thus, the resulting nature of all the solutions is periodic bell wave with at least one kink in the surface depicted by the real part of $\Psi_{17}(x,t)$ in Fig. 9a and square of modulus of $\Psi_{12}(x,t)$ in Fig. 9b. We see that the square of modulus give us many small amplitude waves which can propagate to transmit signal rapidly through

optical fiber. Besides this, the solutions $\Psi_{14,15}(x,t)$ have the same properties that they exhibits muti-peaked optical solitonic nature in presence of singularities. This character is displayed in Fig. 9c via $|\Psi_{14}(x,t)|^2$. The solutions $\Psi_{18,19}(x,t)$ have the same properties that they exhibits dark bell optical soliton in presence of singularities. This character is displayed in Fig. 9d via $|\Psi_{18}(x,t)|^2$.

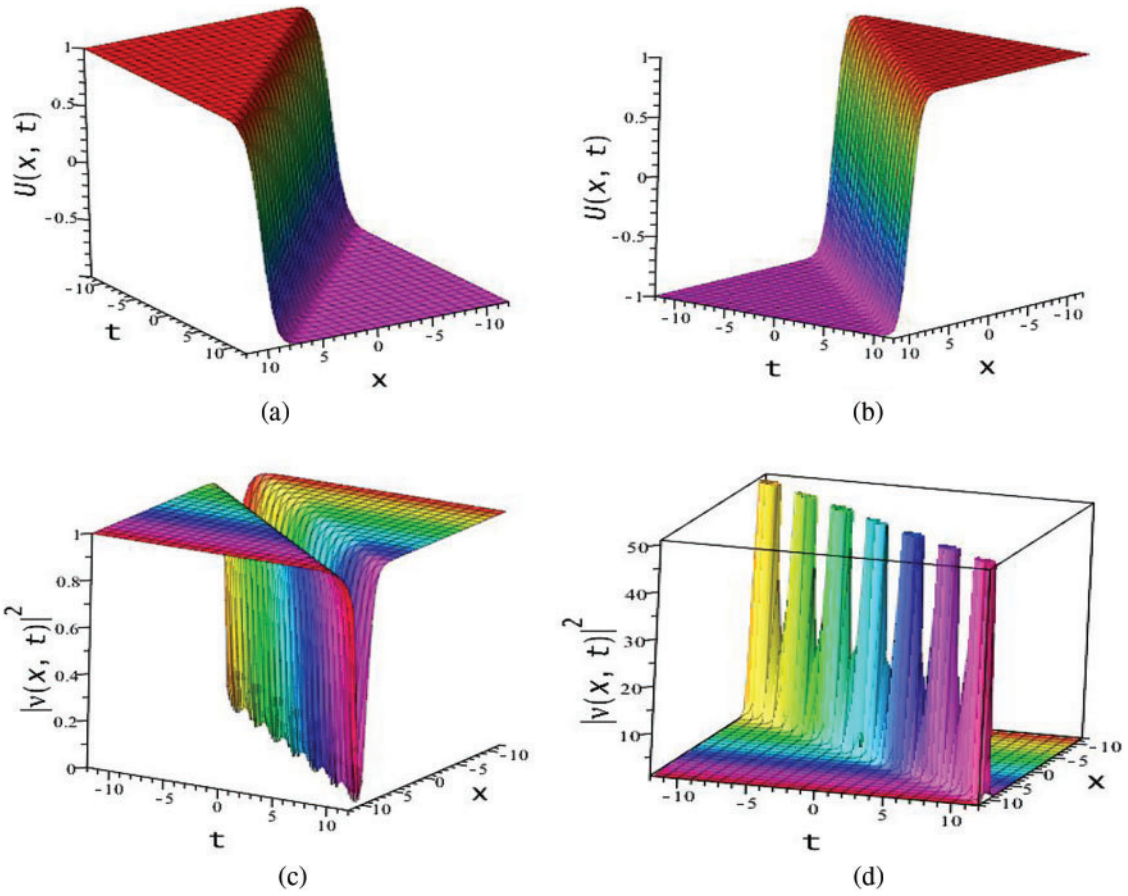

Figure 8: (a) Shock wave (Kink) for + via (*tanh*) of Eq. (44), (b) Shock wave (anti-kink) for−via (*tanh*) of Eq. (44), (c) Optical dark peakon via (*tanh*) of Eq. (44) and (d) Optical bright peaked (anti-peakon) with singularities Eq. (45) for the parametric values $a_1 = 5, a_2 = b_1 = b_2 = h = 2, b_1 = \delta = k = \varepsilon = 1, w = 0.5, \vartheta = -2, L_1 = 2, M_1 = 1$

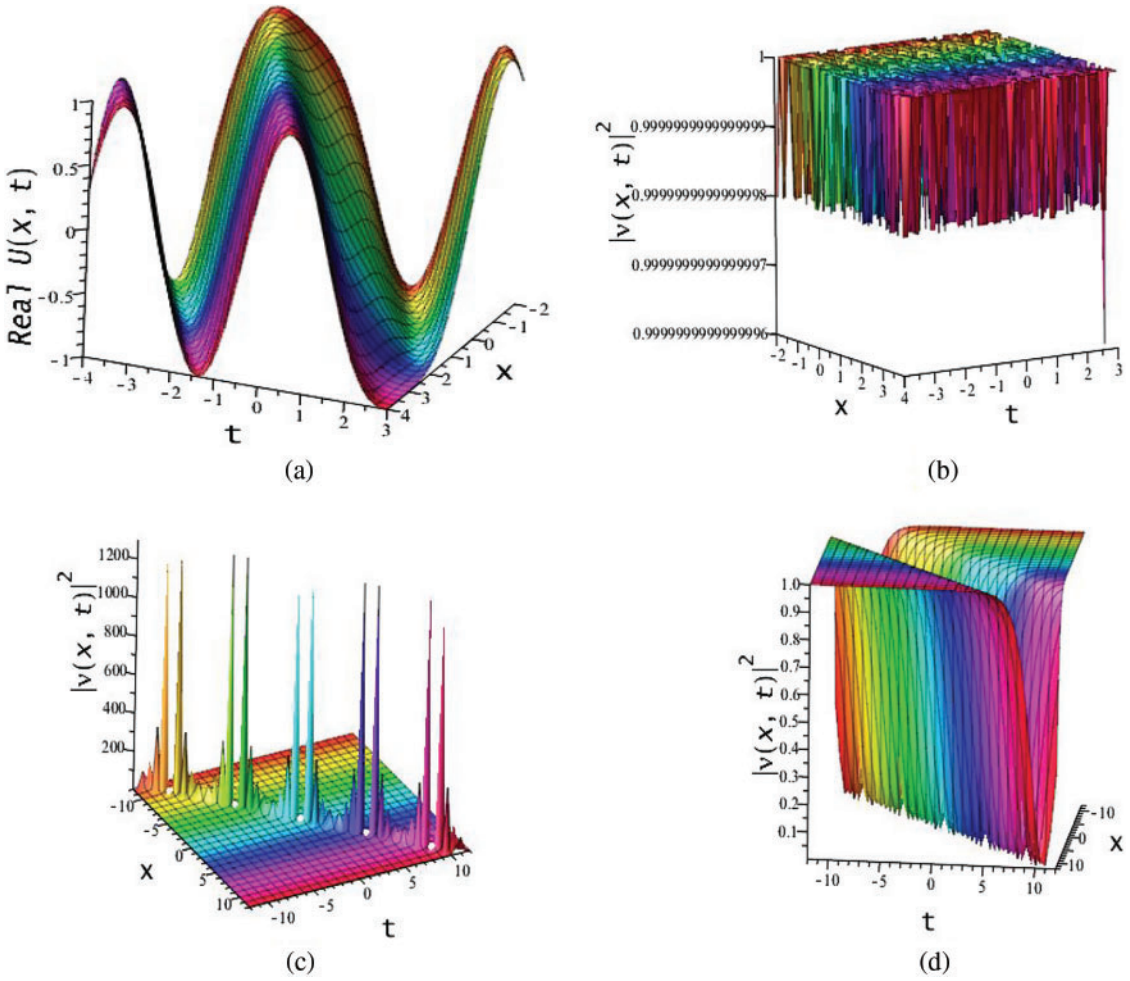

Figure 9: (a) Combine bell kink soliton comes from real part of $|\Psi_{17}(x,t)|$, (b) Small amplitude response $|\Psi_{12}(x,t)|^2$, (c) Multi-peaked optical soliton with singularities via $\Psi_{14}(x,t)$ and (d) Dark bell optical soliton with singularities via $\Psi_{18}(x,t)$ for the parametric values $a_1 = 5, a_2 = b_2 = 2$, $b_1\delta = k = \varepsilon = M_1 = 1, w = 0.5, \vartheta = -2$

2.5 Optical Soliton Solutions to the Biswas-Arshed Model via the GK Method

The GK method [30] is a unique approach to obtaining the generalized solitons and periodic rogue waves of the nonlinear evolution equations (NLEEs) [20,21]. We now consider a rational series in this method as:

$$\Psi(\zeta) = \frac{\sum_{r=0}^{n} M_r (F(\zeta))^r}{\sum_{l=0}^{m} L_l (F(\zeta))^l}, \tag{50}$$

where M_r, L_l, are constants to be later calculated and $M_n \neq 0, L_m \neq 0$. The function $F(\zeta)$ satisfies the Ricatti equation,

$$F'(\zeta) = F^2(\zeta) - F(\zeta), \tag{51}$$

with the solution

$$F(\zeta) = \frac{1}{1 + he^{\zeta}}, \tag{52}$$

where h is the integral constant.

The trail solution Eq. (50) to the BAM takes the following form for the balance numbers $n = 2$ and $m = 1$,

$$\Phi(\zeta) = \frac{M_0 + M_1 F(\zeta) + M_2 (F(\zeta))^2}{L_0 + L_1 F(\zeta)}. \tag{53}$$

Putting Eq. (53) into Eq. (3) along with Eq. (51), we obtain a polynomial of $F(\zeta)$ functions, whose equating coefficients lead to a system of equations, and provide the following set of constraints:

$$\text{Set 1:} \quad \begin{aligned} \delta &= \frac{-\Lambda_1}{L_1^2(2k^3b_2^2 + 3k^2a_2b_2 + ka_2^2 - 2kb_2 - a_2)}, \\ w &= \frac{k(k^2L_1^2b_1 + kL_1^2a_1 + \varepsilon M_1^2 + \vartheta M_1^2)}{L_1^2(k^2b_2 + ka_2 - 1)}, \\ M_0 &= 0, \quad L_0 = 0, \quad M_2 = -2M_1, \end{aligned} \tag{54}$$

where L_1, M_1 are constants and $\Lambda_1 = 2\varepsilon k^3 M_1^2 b_2 + 2k^3\vartheta M_1^2 b_2 - 2k^3 L_1^2 b_1 b_2 + 2\varepsilon k^2 M_1^2 a_2 + 2k^2\vartheta M_1^2 a_2 - 3k^2 L_1^2 a_2 b_1 + \varepsilon k M_1^2 b_2 + k\vartheta M_1^2 b_2 - kL_1^2 a_1 a_2 - 2\varepsilon k M_1^2 - 2k\vartheta M_1^2 + 3kL_1^2 b_1 + L_1^2 a_1$.

$$\text{Set 2:} \quad \begin{aligned} \delta &= \frac{-\Lambda_2}{8L_0^2(k^2b_2 + ka_2 - 1)(2kb_2 + a_2)}, \\ w &= \frac{k(8k^2L_0^2b_1 + 8kL_0^2a_1 - \varepsilon M_1^2 - \vartheta M_1^2)}{8L_0^2(k^2b_2 + ka_2 - 1)}, \\ M_0 &= 0, \quad M_2 = -M_1, \quad L_1 = -2L_0, \end{aligned} \tag{55}$$

where L_0, M_1 are constants and $\Lambda_2 = \varepsilon k^3 M_1^2 b_2 + k^3\vartheta M_1^2 b_2 - 16k^3 L_0^2 b_1 b_2 + \varepsilon k^2 M_1^2 a_2 + k^2\vartheta M_1^2 a_2 - 24k^2 L_0^2 a_2 b_1 - \varepsilon k M_1^2 b_2 - k\vartheta M_1^2 b_2 - 8kL_0^2 a_1 a_2 - \varepsilon k M_1^2 - k\vartheta M_1^2 + 24kL_0^2 b_1 + 8L_0^2 a_1$.

$$\text{Set 3:} \quad \begin{aligned} \delta &= \frac{-\Lambda_3}{2(2k^3b_2^2 + 3k^2a_2b_2 + ka_2^2 - 2kb_2 - a_2)L_0^2}, \\ w &= \frac{k(k^2L_0^2b_1 + kL_0^2a_1 + \varepsilon M_0^2 + \vartheta M_0^2)}{L_0^2(k^2b_2 + ka_2 - 1)}, \\ M_1 &= -2M_0, \quad M_2 = 2M_0, \quad L_1 = -2L_0, \end{aligned} \tag{56}$$

where L_0, M_0 are constants and $\Lambda_3 = \varepsilon k^3 M_0^2 b_2 + k^3\vartheta M_0^2 b_2 - 4k^3 L_0^2 b_1 b_2 + \varepsilon k^2 M_0^2 a_2 + k^2\vartheta M_0^2 a_2 - 6k^2 L_0^2 a_2 b_1 + 2\varepsilon k M_0^2 b_2 + 2k\vartheta M_0^2 b_2 - 2kL_0^2 a_1 a_2 - \varepsilon k M_0^2 - k\vartheta M_0^2 + 6kL_0^2 b_1 + 2L_0^2 a_1$.

$$\text{Set 4:} \quad \begin{aligned} \delta &= \frac{-\Lambda_4}{(2k^3b_2^2 + 3k^2a_2b_2 + ka_2^2 - 2kb_2 - a_2)L_0^2}, \\ w &= \frac{k(k^2L_0^2b_1 + kL_0^2a_1 + \varepsilon M_0^2 + \vartheta M_0^2)}{L_0^2(k^2b_2 + ka_2 - 1)}, \\ M_1 &= \frac{M_0(L_1 - 2L_0)}{L_0}, M_2 = -\frac{M_0 L_1}{L_0}, \end{aligned} \tag{57}$$

where L_0, L_1, M_0 are constants and $\Lambda_4 = 2\varepsilon k^3 M_0^2 b_2 + 2k^3 \vartheta M_0^2 b_2 - 2k^3 L_0^2 b_1 b_2 + 2\varepsilon k^2 M_0^2 a_2 + 2k^2 \vartheta M_0^2 a_2 - 3k^2 L_0^2 a_2 b_1 + \varepsilon k M_0^2 b_2 + k\vartheta M_0^2 b_2 - k L_0^2 a_1 a_2 - 2\varepsilon k M_0^2 - 2k\vartheta M_0^2 + 3k L_0^2 b_1 + L_0^2 a_1$.

Now for the Set 1, if we combine Eq. (54) with Eq. (53) and substituting into Eq. (2), we obtain the exact soliton solutions of Eq. (1). These solutions are able to give us optical rogue wave solitons,

$$\Psi_{20}(x,t) = \frac{M_1}{L_1} F(x-\delta t) e^{i(-kx+wt+\rho)}, \tag{58}$$

where δ and w come from Eq. (54) and $F(x-\delta t)$ comes from Eq. (52).

The behavior of the solution $\Psi_{20}(x,t)$ via Eq. (58) comes from produce periodic exponential function and exponential function (give solitonic nature). Thus, the resulting nature of the solution is periodic wave with a single shock (anti-kink) wave in both the real and imaginary parts, illustrated in Figs. 10b and 10c. But the simple $\Phi(x,t)$ and square of modulus of $\Psi_{20}(x,t)$ exhibits anti-kink type shock wave response in Figs. 10a and 10b, respectively.

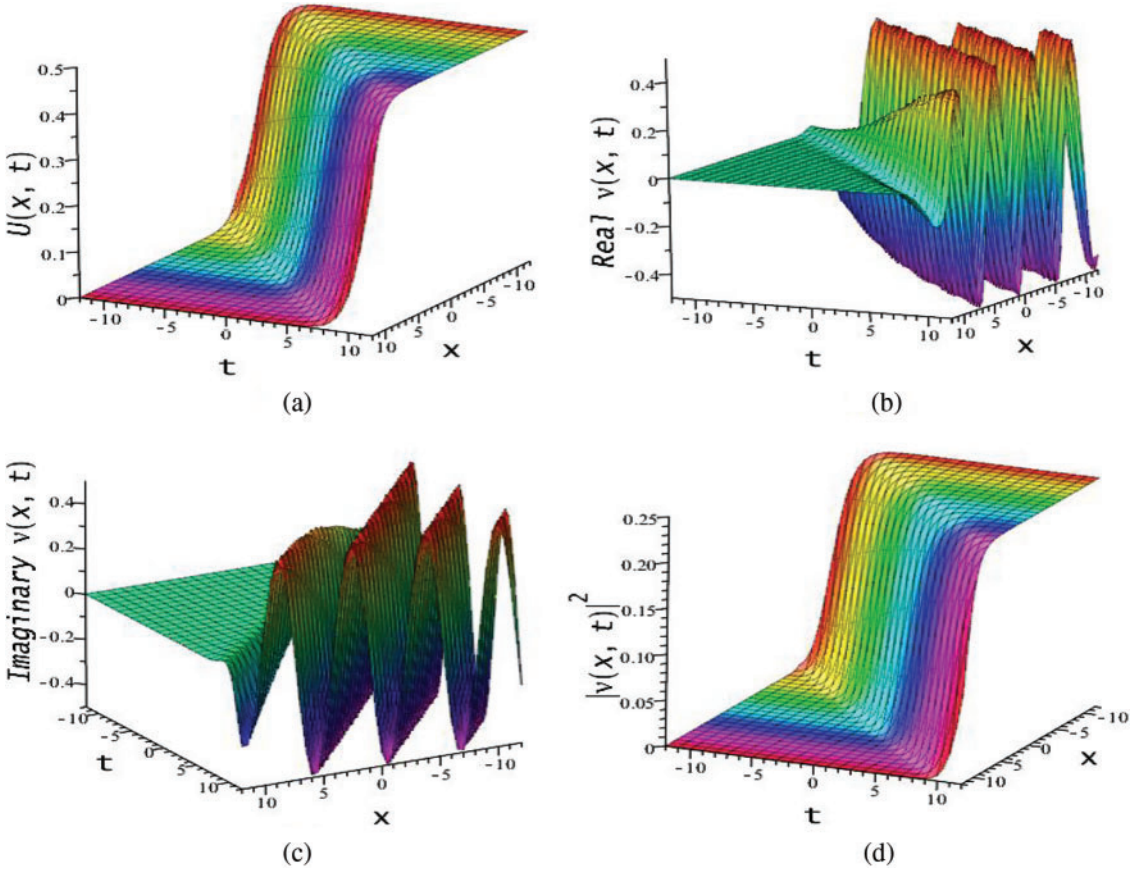

Figure 10: (a) Shock wave, (b) Real part of, (c) Imaginary part of and (d) Shock wave of Eq. (58) for the parametric values $a_1 = a_2 = b_1 = \delta = k = \varepsilon = 1, b_2 = h = 2, w = 0.5, \vartheta = -2, L_1 = 2, M_1 = 1$

Similar, for the Set 2, if we combine Eq. (55) with Eq. (53) and substituting into Eq. (2), we obtain the exact soliton solutions of Eq. (1). These solutions lead to optical rogue wave solitons,

$$\Psi_{21}(x,t) = \frac{M_1 F(x-\delta t)(1-F(x-\delta t))}{L_0\{1-2F(x-\delta t)\}} e^{i(-kx+wt+\rho)}, \tag{59}$$

where δ and w come from Eq. (55) and $F(x-\delta t)$ from Eq. (52). For the Set 3, if we combine Eq. (56) with Eq. (53) and substituting into Eq. (2), we obtain the optical rogue wave soliton solutions of Eq. (1),

$$\Psi_{22}(x,t)=\frac{M_0\{1-2F(x-\delta t)+2(F(x-\delta t))^2\}}{L_0\{1-2F(x-\delta t)\}}e^{i(-kx+wt+\rho)}, \tag{60}$$

where δ and w come from Eq. (56), and $F(x-\delta t)$ from Eq. (52). And for the Set 4, combining Eq. (57) with Eq. (53) and substituting into Eq. (2), we obtain the optical rogue wave soliton solutions of Eq. (1),

$$\Psi_{23}(x,t)=\frac{M_0L_0+M_0(L_1-2L_0)F(x-\delta t)-M_0L_1(F(x-\delta t))^2}{L_0^2\{1-2F(x-\delta t)\}}e^{i(-kx+wt+\rho)}, \tag{61}$$

where δ and w come from Eq. (57) and $F(x-\delta t)$ from Eq. (52). The behavior of the solution $\Psi_{21}(x,t)$, $\Psi_{22}(x,t)$ and $\Psi_{23}(x,t)$ are same with singularities arises for $L_0=0$ or $\{1-2F(x-\delta t)\}=0$. Since the resulting solution via Eqs. (59)–(61) comes from produce periodic exponential function and exponential function (give solitonic nature). Here, we reveal the results of Eq. (61) only against the three solutions, which exhibits a periodic wave with a singular shock wave in the both real and imaginary parts, illustrated in Fig. 11b and 11c. But the simple $\Phi(x,t)$ presents singular kink type shock wave (Fig. 11a) and the square of modulus of $\Psi_{23}(x,t)$ exhibits multi-peaked optical soliton with more singularities (Fig. 11d).

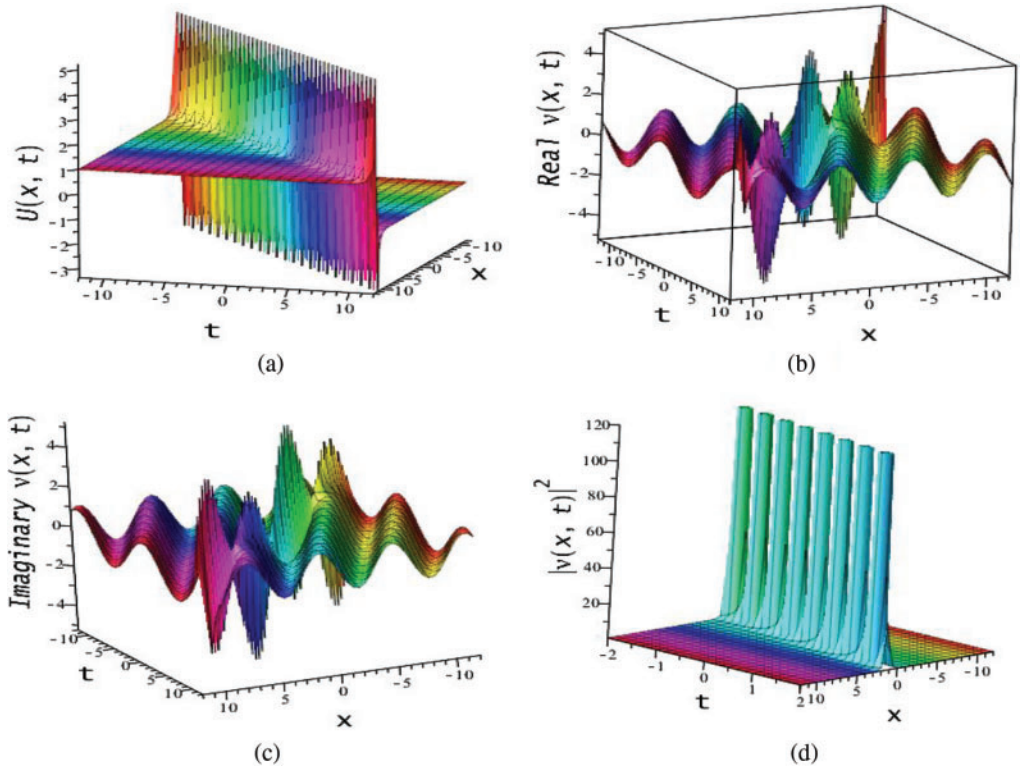

Figure 11: (a) Shock wave with singularity, (b) Real part of, (c) Imaginary part of and (d) Singular bright soliton of Eq. (61) for the parametric values $a_1=a_2=b_1=\delta=k=\varepsilon=1, b_2=h=2, w=0.5, \vartheta=-2, L_0=M_0=1$

3 Results and Discussions

This section will provide some discussions of the physical importance of the acquired results. The results of the BAM structure presented in this research have richer physical structure than earlier outcomes in the literature [11–18]. The recorded solutions are significant in the context of nonlinear dynamics, physical science, mathematical physics and the optical communication through optical fiber. We studied BAM given by Eq. (1) using bifurcation analysis, dynamical system, EShGEE and GK schemes. The bifurcation scheme provided us the evidence of the existence of various periodic wave and optical soliton solution splitting parametric areas shown in different phase portraits in Figs. 1 and 3 of the BAM. We also illustrated the physical meaning of the obtained explicit solutions 3D and contour plots that appeared in Figs. 4 and 11.

4 Conclusion

The main results of this paper are on the application of the bifurcation analysis via a dynamical system scheme and the derivation of all bounded optical wave solutions of the Biswas-Arshed model. We obtained all types of phase portraits and corresponding bounded optical shock wave, bounded solitary wave, and the bounded periodic wave solutions of the BAM by using the dynamical scheme, the extended sinh-Gordon equation expansion, and the generalized Kudryashov integral schemes. To our knowledge, these types of solitons for the Biswas-Arshed model have not been explored before [13–16,19]. All the solutions are illustrated graphically. The model could be investigated to get multi-soliton and rogue wave solutions by the other existing methods, in particular, Hirota bilinear approach [24,25] and Darboux transformation [26]. The results would be interesting to use in social media, telecommunication industries, internet zone, and many other aspects.

Acknowledgement: The authors thank to Prof. Ji-Huan He for his valuable suggestions that helped us in improving the quality and presentation of this paper.

Funding Statement: This research was supported by the Deanship of Scientific Research, Prince Sattam bin Abdulaziz University, Alkharj, Saudi Arabia, under Grant No. 2021/01/19122.

Conflicts of Interest: The authors declare that they have no conflicts of interest to report regarding the present study.

References

1. Agrawal, G. P. (2000). Nonlinear fiber optics. In: *Nonlinear science at the dawn of the 21st century*, pp. 195–211. Springer.
2. Haus, H. A., Wong, W. S. (1996). Solitons in optical communications. *Reviews of Modern Physics, 68(2),* 423. DOI 10.1103/RevModPhys.68.423.
3. Zhao, L. C., Li, S. C., Ling, L. (2016). W-shaped solitons generated from a weak modulation in the Sasa-Satsuma equation. *Physical Review E, 93(3),* 032215. DOI 10.1103/PhysRevE.93.032215.
4. Biswas, A., Yildirim, Y., Yasar, E., Zhou, Q., Moshokoa, S. P. et al. (2018). Optical solitons for lakshmanan–Porsezian–Daniel model by modified simple equation method. *Optik, 160,* 24–32. DOI 10.1016/j.ijleo.2018.01.100.
5. Biswas, A., Yildirim, Y., Yasar, E., Triki, H., Alshomrani, A. S. et al. (2018). Optical soliton perturbation for complex Ginzburg–Landau equation with modified simple equation method. *Optik, 158,* 399–415. DOI 10.1016/j.ijleo.2017.12.131.

6. Mirzazadeh, M., Yıldırım, Y., Yaşar, E., Triki, H., Zhou, Q. et al. (2018). Optical solitons and conservation law of Kundu–Eckhaus equation. *Optik, 154,* 551–557. DOI 10.1016/j.ijleo.2017.10.084.
7. Biswas, A., Yildirim, Y., Yasar, E., Zhou, Q., Mahmood, M. F. et al. (2018). Optical solitons with differential group delay for coupled Fokas–Lenells equation using two integration schemes. *Optik, 165,* 74–86. DOI 10.1016/j.ijleo.2018.03.100.
8. Biswas, A., Yıldırım, Y., Yaşar, E., Zhou, Q., Moshokoa, S. P. et al. (2018). Sub pico-second pulses in mono-mode optical fibers with Kaup–Newell equation by a couple of integration schemes. *Optik, 167,* 121–128. DOI 10.1016/j.ijleo.2018.04.063.
9. Biswas, A., Yildirim, Y., Yasar, E., Mahmood, M. F., Alshomrani, A. S. et al. (2018). Optical soliton perturbation for Radhakrishnan–Kundu–Lakshmanan equation with a couple of integration schemes. *Optik, 163,* 126–136. DOI 10.1016/j.ijleo.2018.02.109.
10. Biswas, A., Yildirim, Y., Yasar, E., Zhou, Q., Moshokoa, S. P. et al. (2018). Optical soliton perturbation with resonant nonlinear Schrödinger's equation having full nonlinearity by modified simple equation method. *Optik, 160,* 33–43. DOI 10.1016/j.ijleo.2018.01.098.
11. Biswas, A., Arshed, S. (2018). Optical solitons in presence of higher order dispersions and absence of self-phase modulation. *Optik, 174,* 452–459. DOI 10.1016/j.ijleo.2018.08.037.
12. Yildirim, Y. (2019). Optical solitons of Biswas–Arshed equation by trial equation technique. *Optik, 182,* 876–883. DOI 10.1016/j.ijleo.2019.01.084.
13. Yildirim, Y. (2019). Optical solitons of Biswas-Arshed equation by modified simple equation technique. *Optik, 182,* 986–994. DOI 10.1016/j.ijleo.2019.01.106.
14. Tahir, M., Awan, A. U. (2020). Optical travelling wave solutions for the Biswas–Arshed model in kerr and non-kerr law media. *Pramana, 94(1),* 1–8. DOI 10.1007/s12043-019-1888-y.
15. Tahir, M., Awan, A., Rehman, H. (2019). Dark and singular optical solitons to the Biswas–Arshed model with Kerr and power law nonlinearity. *Optik, 185,* 777–783. DOI 10.1016/j.ijleo.2019.03.108.
16. Rehman, H. U., Saleem, M. S., Zubair, M., Jafar, S., Latif, I. (2019). Optical solitons with Biswas–Arshed model using mapping method. *Optik, 194,* 163091. DOI 10.1016/j.ijleo.2019.163091.
17. Ekici, M., Sonmezoglu, A. (2019). Optical solitons with Biswas-Arshed equation by extended trial function method. *Optik, 177,* 13–20. DOI 10.1016/j.ijleo.2018.09.134.
18. Aouadi, S., Bouzida, A., Daoui, A., Triki, H., Zhou, Q. et al. (2019). W-shaped, bright and dark solitons of Biswas–Arshed equation. *Optik, 182,* 227–232. DOI 10.1016/j.ijleo.2019.01.027.
19. Hoque, M. F. (2020). Optical soliton solutions of the Biswas–Arshed model by the $\tan(\Sigma/2)$ expansion approach. *Physica Scripta, 95(7),* 075219. DOI 10.1088/1402-4896/ab97ce.
20. Arnous, A. H., Mirzazadeh, M. (2016). Application of the generalized Kudryashov method to the Eckhaus equation. *Nonlinear Analysis: Modelling and Control, 21(5),* 577–586. DOI 10.15388/NA.2016.5.1.
21. Ullah, M. S., Ali, M. Z., Rahman, Z. (2019). Novel exact solitary wave solutions for the time fractional generalized Hirota–Satsuma coupled kdV model through the generalized Kudryshov method. *Contemporary Mathematics*, *1*, 25–32. DOI 10.37256/cm.11201936.25-33.
22. Fu, Z., Liu, S., Liu, S. (2006). Exact jacobian elliptic function solutions to sinh-Gordon equation. *Communications in Theoretical Physics, 45(1),* 55. DOI 10.1088/0253-6102/45/1/010.
23. Yang, X., Tang, J. (2008). Travelling wave solutions for Konopelchenko–Dubrovsky equation using an extended sinh-gordon equation expansion method. *Communications in Theoretical Physics, 50(5),* 1047. DOI 10.1088/0253-6102/50/5/06.
24. Harun, R., Ma, W. (2018). Dynamics of mixed lump-solitary waves of an extended (2+1)-dimensional shallow water wave model. *Physics Letters A, 382(45),* 3262–3268. DOI 10.1016/j.physleta.2018.09.019.
25. Wang, X. B., Tian, S. F., Qin, C. Y., Zhang, T. T. (2017). Characteristics of the solitary waves and rogue waves with interaction phenomena in a generalized (3+1)-dimensional Kadomtsev–Petviashvili equation. *Applied Mathematics Letters, 72,* 58–64. DOI 10.1016/j.aml.2017.04.009.

26. Bagrov, V. G., Samsonov, B. F. (1997). Darboux transformation and elementary exact solutions of the Schrödinger equation. *Pramana, 49(6),* 563–580. DOI 10.1007/BF02848330.
27. Nemytskii, V. V. (2015). *Qualitative theory of differential equations*. USA: Princeton University Press.
28. He, J. H., Hou, W. F., He, C. H., Saeed, T., Hayat, T. (2021). Variational approach to fractal solitary waves. *Fractals, 29(7),* 2150199. DOI 10.1142/S0218348X21501991.
29. He, J. H., He, C. H., Saeed, T. (2021). A fractal modification of Chen–Lee–Liu equation and its fractal variational principle. *International Journal of Modern Physics B, 35(21),* 2150214. DOI 10.1142/S0217979221502143.
30. Ullah, N., Asjad, M. I., Iqbal, A., Rehman, H. U., Hassan, A. et al. (2021). Analysis of optical solitons solutions of two nonlinear models using analytical technique. *AIMS Mathematics, 6(12),* 13258–13271. DOI 10.3934/math.2021767.